

1 Functional MRI brain state 2 occupancy in the presence of 3 cerebral small vessel disease – 4 pre-registration for a replication 5 analysis of the Hamburg City Health 6 Study

✉ For correspondence:
e.schlemm@uke.de

Present address:
Dr. Dr. Eckhard Schlemm,
Klinik und Poliklinik für
Neurologie,
Universitätsklinikum
Hamburg-Eppendorf,
Martinistr. 52,
D-20251 Hamburg

Data availability:
Preprocessed data will be
available e.g. on
<https://github.com/csi-hamburg/HCHS-brain-states-RR>.

Funding: Deutsche
Forschungsgemeinschaft
(DFG) - 178316478 - C2

Competing interests: The
author declares no
competing interests.

7 **Eckhard Schlemm, MBBS PhD^①✉ and Thies Ingwersen, MD¹**

8 ¹Department of Neurology, University Medical Center
9 Hamburg-Eppendorf

11 **Abstract**

12 **Objective:** To replicate recent findings about the association between the extent of
13 cerebral small vessel disease (cSVD), functional brain network dedifferentiation and
14 cognitive impairment.
15 **Methods:** We will analyze demographic, imaging and behavioral data from the
16 prospective population-based Hamburg City Health Study. Using a fully prespecified
17 analysis pipeline, we will estimate discrete brain states from structural and resting-state
18 functional magnetic resonance imaging (MRI). In a multiverse analysis we will vary brain
19 parcellations and functional MRI confound regression strategies. Severity of cSVD will
20 be operationalised as the volume of white matter hyperintensities of presumed
21 vascular origin. Processing speed and executive dysfunction are quantified by the trail
22 making test (TMT).
23 **Hypotheses:** We hypothesize a) that greater volume of supratentorial white matter

²⁴ hyperintensities is associated with less time spent in functional MRI-derived brain
²⁵ states of high fractional occupancy; and b) that less time spent in these high-occupancy
²⁶ brain states is associated with longer time to completion in part B of the TMT.

²⁷

²⁸ Introduction

²⁹ Cerebral small vessel disease (cSVD) is an arteriolopathy of the brain, associated with
³⁰ age and common cardiovascular risk factors (Wardlaw, C. Smith, and Dichgans, 2013).
³¹ cSVD predisposes to ischemic, in particular lacunar, stroke and may lead to cognitive im-
³² pairment and dementia (Cannistraro et al., 2019). Neuroimaging findings in cSVD reflect
³³ its underlying pathology (Wardlaw, Valdés Hernández, and Muñoz-Maniega, 2015) and
³⁴ include white matter hyperintensities (WMH) and lacunes of presumed vascular origin,
³⁵ small subcortical infarcts and microbleeds, enlarged perivascular spaces as well as brain
³⁶ atrophy (Wardlaw, E. E. Smith, et al., 2013). However, the extent of visible cSVD features
³⁷ on magnetic resonance imaging (MRI) is an imperfect predictor of the severity of clini-
³⁸ cal sequelae (Das et al., 2019), and our understanding of the causal mechanisms linking
³⁹ cSVD-associated brain damage to clinical deficits remains limited (Bos et al., 2018).

⁴⁰ Recent efforts have concentrated on exploiting network aspects of the structural (Tu-
⁴¹ ladhar, Dijk, et al., 2016; Tuladhar, Tay, et al., 2020; Lawrence, Zeestraten, et al., 2018)
⁴² and functional (Dey et al., 2016; Schulz et al., 2021) organization of the brain to under-
⁴³ stand the relation between cSVD and clinical deficits in cognition and other domains re-
⁴⁴ liant on distributed processing. Reduced structural network efficiency has repeatedly
⁴⁵ been described as a causal factor in the development of cognitive impairment, in partic-
⁴⁶ ular executive dysfunction und reduced processing speed, in cSVD (Lawrence, Chung,
⁴⁷ et al., 2014; Shen et al., 2020; Reijmer et al., 2016; Prins et al., 2005). Findings with
⁴⁸ respect to functional connectivity results(FC), on the other hand, are more heteroge-
⁴⁹ neous, perhaps due to its limited reproducibility in than their SC counterparts, perhaps
⁵⁰ because FC measurements are prone to be affected by hemodynamic factors and noise,
⁵¹ resulting in relatively low reliability, especially with resting-state scans of short duration
⁵² (Laumann, Gordon, et al., 2015). This problem is exacerbated in the presence of cSVD
⁵³ and dependence on made worse by the arbitrary processing choices (Lawrence, Tozer,
⁵⁴ et al., 2018; Gesierich et al., 2020).

⁵⁵ As a promising new avenue, time-varying, or dynamic, functional connectivity approaches

56 have more recently been explored in patients with subcortical ischemic vascular disease
57 (Yin et al., 2022; Xu et al., 2021). While the study of dynamic FC measures may not
58 solve the problem of limited reliability, especially in small populations or subjects with
59 extensive structural brain changes, it adds another – temporal – dimension to the study of
60 functional brain organisation, which is otherwise overlooked. Importantly, FC dynamics
61 do not only reflect moment-to-moment fluctuations in cognitive processes but are also
62 related to brain plasticity and homeostasis (Laumann and Snyder, 2021; Laumann, Snyder,
63 et al., 2017), which may be impaired in cSVD.

64 In the present paper, we aim to replicate and extend the main results of (Schlemm et
65 al., 2022); in this recent study, the authors analyzed MR imaging and clinical data from the
66 prospective Hamburg City Health Study (HCHS, Jagodzinski et al., 2020) using a coacti-
67 vation pattern approach to define discrete brain states and found associations between
68 the WMH load, time spent in high-occupancy brain states characterized by activation
69 or suppression of the default mode network (DMN) and ~~executive dysfunction~~cognitive
70 impairment.

71 The fractional occupancy of a functional MRI-derived discrete brain state is a subject-specific
72 measure of brain dynamics defined as the proportion of BOLD volumes assigned to that
73 state relative to all BOLD volumes acquired during a resting-state scan.

74 Our primary hypothesis is that the volume of supratentorial white matter hyperinten-
75 sities is associated with the fractional occupancy (~~defined below~~) of DMN-related brain
76 states in a middle-aged to elderly population mildly affected by cSVD. Our second hy-
77 pothesis is that this fractional occupancy is associated with executive dysfunction and
78 reduced processing speed, measured as the time to complete part B of the trail making
79 test (TMT).

80 Both hypotheses will be tested in an independent subsample of the HCHS study popu-
81 lation using the same imaging protocols, examination procedures and analysis pipelines
82 as in (Schlemm et al., 2022). The robustness of associations will be explored in a multi-
83 verse approach by varying key steps in the analysis pipeline.

84 Methods

85 Study population

86 The paper will analyze data from the Hamburg City Health Study (HCHS), which is an
87 ongoing prospective, population-based cohort study aiming to recruit a cross-sectional

Question	Hypothesis	Sampling plan	Analysis plan	Rationale deciding sensitivity for the test	Interpretation given different outcomes	Theory that could be shown wrong by the outcome
Is severity of cerebral small vessel disease, quantified by the volume <u>of</u> supratentorial white matter hyperintensities of presumed vascular origin (WMH), associated with time spent in high-occupancy brain states, defined by resting-state functional MRI	Higher WMH volume is associated with lower average occupancy of the two highest-occupancy brain states.	Available subjects with clinical and imaging data from the <u>the</u> HCHS (Jagodzinski et al., 2020)	Standardized preprocessing of structural and functional MRI data • automatic quantification of WMH • co-activation pattern analysis • multivariable generalised regression analyses	Tradition	$P < 0.05 \rightarrow$ rejection of the null hypothesis of no association between cSVD and fractional occupancy; $P > 0.05 \rightarrow$ insufficient evidence to reject the null hypothesis	Functional brain dynamics are not related to subcortical ischemic vascular disease.

Table 1. Study Design Template

⁸⁸ sample of 45 000 adult participants from the city of Hamburg, Germany (Jagodzinski et
⁸⁹ al., 2020). From the first 10 000 participants of the HCHS we will aim to include those
⁹⁰ who were documented to have received brain imaging (n=2652) and exclude those who
⁹¹ were analyzed in our previous report (Schlemm et al., 2022). The ethical review board of
⁹² the Landesärztekammer Hamburg (State of Hamburg Chamber of Medical Practitioners)
⁹³ approved the HCHS (PV5131), all participants provided written informed consent.

⁹⁴ **Demographic and clinical characterization**

⁹⁵ From the study database we will extract participants' age at the time of inclusion in years,
⁹⁶ their self-reported gender and the number of years spent in education. During the visit
⁹⁷ at the study center, participants undergo cognitive assessment using standardized tests.
⁹⁸ We will extract from the database their performance scores in the Trail Making Test part
⁹⁹ B, measured in seconds, as an operationalization of executive function and psychomotor
¹⁰⁰ processing speed (Tombaugh, 2004; Arbuthnott and Frank, 2000).

¹⁰¹ **MRI acquisition and preprocessing**

¹⁰² The magnetic resonance imaging protocol for the HCHS includes structural and resting-
¹⁰³ state functional sequences. The acquisition parameters on a 3 T Siemens Skyra MRI scan-
¹⁰⁴ ner (Siemens, Erlangen, Germany) have been reported before (Petersen et al., 2020; Frey
¹⁰⁵ et al., 2021) and are given as follows:

¹⁰⁶ For T_1 -weighted anatomical images, a 3D rapid acquisition gradient-echo sequence
¹⁰⁷ (MPRAGE) was used with the following sequence parameters: repetition-repetition time
¹⁰⁸ TR = 2500 ms, echo time TE = 2.12 ms, 256 axial slices, slice thickness ST = 0.94 mm, and
¹⁰⁹ in-plane resolution IPR = $(0.83 \times 0.83) \text{ mm}^2$.

¹¹⁰ T_2 -weighted fluid attenuated inversion recovery (FLAIR) images were acquired with

111 the following sequence parameters: TR = 4700 ms, TE = 392 ms, 192 axial slices, ST =
112 0.9 mm, IPR = $(0.75 \times 0.75) \text{ mm}^2$.

113 125 resting state functional MRI volumes were acquired (TR = 2500 ms; TE = 25 ms;
114 flip angle = 90°; slices = 49; ST = 3 mm; slice gap = 0 mm; IPR = $(2.66 \times 2.66) \text{ mm}^2$). Subjects
115 were asked to keep their eyes open and to think of nothing.

116 We will verify the presence and voxel-dimensions of expected MRI data for each par-
117 ticipant and exclude those for whom at least one of T_1 -weighted, FLAIR and resting-state
118 MRI is missing. We will also exclude participants with a neuroradiologically confirmed
119 space-occupying intra-axial lesion. To ensure reproducibility, no visual quality assess-
120 ment on raw images will be performed.

121 For the remaining participants, structural and resting-state functional MRI data will
122 be preprocessed using FreeSurfer v6.0 (<https://surfer.nmr.mgh.harvard.edu/>), and fmriPrep
123 v20.2.6 (Esteban et al., 2019), using default parameters. Participants will be excluded if
124 automated processing using at least one of these packages fails.

125 Quantification of WMH load

126 For our primary analysis, the extent of ischemic white matter disease will be operational-
127 ized as the total volume of supratentorial WMHs obtained from automated segmentation
128 using a combination of anatomical priors, BIANCA (Griffanti, Zamboni, et al., 2016) and
129 LOCATE (Sundaresan et al., 2019), post-processed with a minimum cluster size of 30 vox-
130 els, as described in (Schlemm et al., 2022). In an exploratory analysis, we partition voxels
131 identified as WMH into deep and periventricular components according to their distance
132 to the ventricular system (cut-off 10 mm, (Griffanti, Jenkinson, et al., 2018))

133 Brain state estimation

134 Output from fMRIprep will be post-processed using xcpEngine v1.2.1 to obtain de-confounded
135 spatially averaged BOLD time series (Circi, Wolf, et al., 2017). For the primary analysis we
136 will use the 36p regression strategy and the Schaefer-400 parcellation (Schaefer et al.,
137 2018), as in (Schlemm et al., 2022).

138 Different atlases and confound regression strategies, as implemented in xcpEngine,
139 will be included in the exploratory multiverse analysis.

140 Co-activation pattern (CAP) analysis will be performed by first aggregating parcellated,
141 de-confounded BOLD signals into a $(n_{\text{parcels}} \times \sum_i n_{\text{time points},i})$ feature matrix, where $n_{\text{time points},i}$
142 denotes the number of retained volumes for subject i after confound regression. Cluster-

¹⁴³ ing will be performed using the k -means algorithm ($k = 5$) with distance measure given
¹⁴⁴ by 1 minus the sample Pearson correlation between points, as implemented in Matlab
¹⁴⁵ R2021a. We will estimate subject- and state-specific fractional occupancies, which are
¹⁴⁶ defined as the proportion of BOLD volumes assigned to each brain state (Vidaurre et al.,
¹⁴⁷ 2018). The two states with the highest average occupancy will be identified as the basis
¹⁴⁸ for further analysis.

¹⁴⁹ Statistical analysis

¹⁵⁰ For demographic (age, gender, years of education) and clinical (TMT-B) variables the num-
¹⁵¹ ber of missing records will be reported. For non-missing values, we will provide descrip-
¹⁵² tive summary statistics using median and interquartile range. The proportion of men
¹⁵³ and women in the sample will be reported. Regression modelling will be carried out as
¹⁵⁴ a complete-case analysis.

¹⁵⁵ As a first outcome-neutral quality check of the implementation of the MRI process-
¹⁵⁶ ing pipeline, brain state estimation and co-activation pattern analysis, we will compare
¹⁵⁷ fractional occupancies between brain states. We expect that the average fractional oc-
¹⁵⁸ cupancy in two high-occupancy states is higher than the average fractional occupancy in
¹⁵⁹ the other three states. Point estimates and 95% confidence intervals will be presented
¹⁶⁰ for the difference in average fractional occupancy to check this assertion.

¹⁶¹ For further analyses, non-zero WMH volumes will be subjected to a logarithmic trans-
¹⁶² formation. Zero values will retain their value zero; to compensate, all models will include
¹⁶³ a binary indicator for zero WMH volume if at least one non-zero value is present.

¹⁶⁴ To assess the primary hypothesis of a negative association between the extent of is-
¹⁶⁵ chemic white matter disease and time spent in high-occupancy brain states, we will per-
¹⁶⁶ form a fixed-dispersion beta-regression to model the logit of the conditional expectation
¹⁶⁷ of the average fractional occupancy of two high-occupancy states as an affine function of
¹⁶⁸ the logarithmized WMH load. Age and gender will be included as covariates. The strength
¹⁶⁹ of the association will be quantified as an odds ratio per interquartile ratio of the WMH
¹⁷⁰ burden distribution and accompanied by a 95% confidence interval. Significance testing
¹⁷¹ of the null hypothesis of no association will be conducted at the conventional significance
¹⁷² level of 0.05. Estimation and testing will be carried out using the 'betareg' package v3.1.4
¹⁷³ in R v4.2.1.

¹⁷⁴ To assess the secondary hypothesis of an association between time spent in high-
¹⁷⁵ occupancy brain states and executive dysfunction, we will perform a generalized linear

176 regression with a Gamma response distribution to model the logarithm of the condi-
177 tional expected completion time in part B of the TMT as an affine function of the average
178 fractional occupancy of two high-occupancy states. Age, gender, years of education and
179 logarithmized WMH load will be included as covariates. The strength of the association
180 will be quantified as a multiplicative factor per percentage point and accompanied by a
181 95% confidence interval. Significance testing of the null hypothesis of no association will
182 be conducted at the conventional significance level of 0.05. Estimation and testing will
183 be carried out using the `glm` function included in the 'stats' package from R v4.2.1.

184 Sample size calculation is based on ~~the data presented in, where an odds ratio of was~~
185 ~~reported as the primary~~ an effect size on the odds ratio scale of 0.95, corresponding to
186 an absolute difference in the probability of occupying a DMN-related brain state between
187 the first and third WMH-load quartile of 1.3 percentage points, and between the 5%
188 95% percentile of 3.1 percentage points. Approximating half the difference in fractional
189 occupancy of DMN-related states between different task demands (rest vs n-back) in
190 healthy subjects, which was estimated to lie between 6 and 7 percentage points (Corn-
191 blath et al., 2020), this value represent a plausible choice for the smallest effect size of
192 interest theoretical and practical interest. It also equals the effect size estimated based
193 on the data presented in (Schlemm et al., 2022).

194 We used simple bootstrapping to create 10 000 hypothetical datasets of size 200, 400,
195 600, 800, 900, 910, ..., 1100, 1200, 1400, 1500, 1600. Each dataset was subjected to the esti-
196 mation procedure described above. For each sample size, the proportion of datasets in
197 which the primary null hypothesis of no association between fractional occupancy and
198 WMH load could be rejected at $\alpha = 0.05$ was computed and is recorded as a power curve
199 in Figure 1.

200 It is seen that a sample size of 960 would allow replication of the reported effect with
201 a power of 80.2 %. We anticipate a sample size of 1500, which yields a power of 93.9 %.

202 Multiverse analysis

203 Both in (Schlemm et al., 2022) and for our primary replication analysis we made certain
204 analytical choices in the operationalisation of brain states and ischemic white matter dis-
205 ease, namely the use of the 36p confound regression strategy, the Schaefer-400 parcella-
206 tion and a BIANCA/LOCATE-based WMH segmentation algorithm. ~~If the hypothesized~~ The
207 robustness of the association between WMH burden and time spent in high-occupancy
208 states ~~can be replicated using these primary analytical choices, its robustness~~ with regard

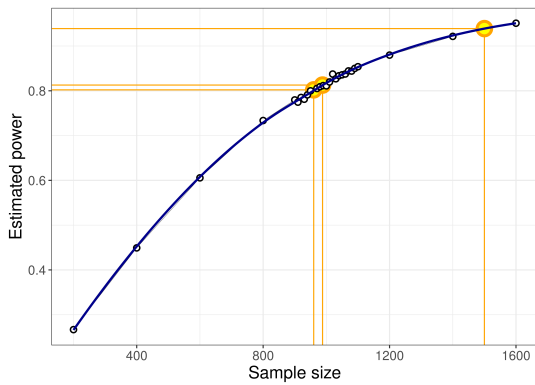


Figure 1. Estimated power for different sample sizes is obtained as the proportion of synthetic data sets in which the null hypothesis of no association between WMH volume and time spent in high-occupancy brain states can be rejected at the $\alpha = 0.05$ significance level. Proportions are based on a total of 10 000 synthetic data sets obtained by bootstrapping the data presented in (Schlemm et al., 2022). Highlighted in orange are the smallest sample size ensuring a power of at least 80 % ($n = 960$), the sample size of the pilot data ($n = 988$, post-hoc power 81.3 %), and the expected sample sample size for this replication study ($n = 1500$, a-priori power 93.9 %).

Name of the atlas	#parcels	Reference
Desikan-Killiany	86	Desikan et al., 2006
AAL	116	Tzourio-Mazoyer et al., 2002
Harvard-Oxford	112	Makris et al., 2006
glasser360	360	Glasser et al., 2016
gordon333	333	Gordon et al., 2016
power264	264	Power, Cohen, et al., 2011
schaefner{N}	100	Schaefer et al., 2018
	200	
	400	

AAL: Automatic Anatomical Labelling

(a) Parcellations

Design	Reference
24p	Friston et al., 1996
24p + GSR	Macey et al., 2004
36p	Satterthwaite et al., 2013
26p <ins>36p</ins> + spike regression	Cox, 1996
36p + despiking	Satterthwaite et al., 2013
36p + scrubbing	Power, Mitra, et al., 2014
aCompCor	Muschelli et al., 2014
tCompCor	Behzadi et al., 2007
AROMA	Pruim et al., 2015

GSR: Global signal regression, AROMA: bla
Automatic Removal of Motion Artifacts

(b) Confound regression strategies, adapted from (Circic, Wolf, et al., 2017)

Table 2. Multiverse analysis, implemented using xcpEngine (Circic, Rosen, et al., 2018)

209 to other choices will be explored in a multiverse analysis (Steegen et al., 2016). Specifically,
 210 in an exploratory analysis, we will estimate brain states from BOLD time series
 211 processed according to a variety of established confound regression strategies and ag-
 212 gregated over different cortical brain parcellations (Table 2, Circic, Rosen, et al., 2018; Circic,
 213 Wolf, et al., 2017). Extent of cSVD will additionally be quantified by the volume of deep
 214 and periventricular white matter hyperintensities.
 215 For each combination of analytical choice of confound regression strategy, parcella-
 216 tion and subdivision of white matter lesion load ($9 \times 9 \times 3 = 243$ scenarios in total) we will
 217 quantify the association between WMH load and average time spent in high-occupancy
 218 brain states using odds ratio and 95 % confidence intervals as described above.
 219 No hypothesis testing and ~~, therefore, no adjustment for multiple testing,~~ will be
 220 carried out in these ~~non-primary analyses~~, multiverse analyses. They rather serve to

221 inform about the robustness of the outcome of the test of the primary hypothesis. Any
222 substantial conclusions about the association between severity of cerebral small pathology
223 and time spent in high-occupancy brain states, as stated in the Scientific Question in
224 Table 1, will be drawn from the primary analysis using pre-specified methodological choices.

225

226 **Exploratory-Further exploratory analysis**

227 In previous work, two high-occupancy brain states were related to the default-mode net-
228 work (Cornblath et al., 2020). We will further explore this relation by computing, for each
229 individual brain state, the cosine similarity of the positive and negative activations of
230 the cluster's centroid with a set of a-priori defined functional 'communities' or networks
231 (Schaefer et al., 2018; Yeo et al., 2011). Results will be thus visualized as spider plots for
232 the Schaefer, Gordon and Power atlases.

233 In further exploratory analyses we plan to describe the associations between brain
234 state dynamics and other measures of cognitive ability, such as memory and language.

235 **Code and pilot data**

236 Summary data from the first 1000 imaging data points of the HCHS have been published
237 with (Schlemm et al., 2022) and form the basis for the hypotheses tested in this replication
238 study. We have implemented our prespecified analysis pipeline described above in R
239 and Matlab, and applied it to this previous sample. Data, code and results have been
240 stored on GitHub (https://github.com/csi-hamburg/HCHS_brain_states_RR) und preserved
241 on Zenodo.

242 Thus re-analysing data from 988 subjects, the separation between two high-occupancy
243 and three low-occupancy brain states could be reproduced for all combinations of brain
244 parcellation and confound regression strategies (Figure 2).

245 In a multiverse analysis, the main finding was somewhat robust with respect to these
246 choices: a statistically significant negative association between WMH load and time spent
247 in high-occupancy states was observed in 18/81 scenarios, with 5/81 statistically signifi-
248 cant positive associations occurring with the Desikan-Killiany parcellation only (Figure 3).

249 The secondary finding of an association between greater TMT-B times and lower frac-
250 tional occupancy was similarly robust with 12/81 statistically significant negative and no
251 statistically significant positive associations.

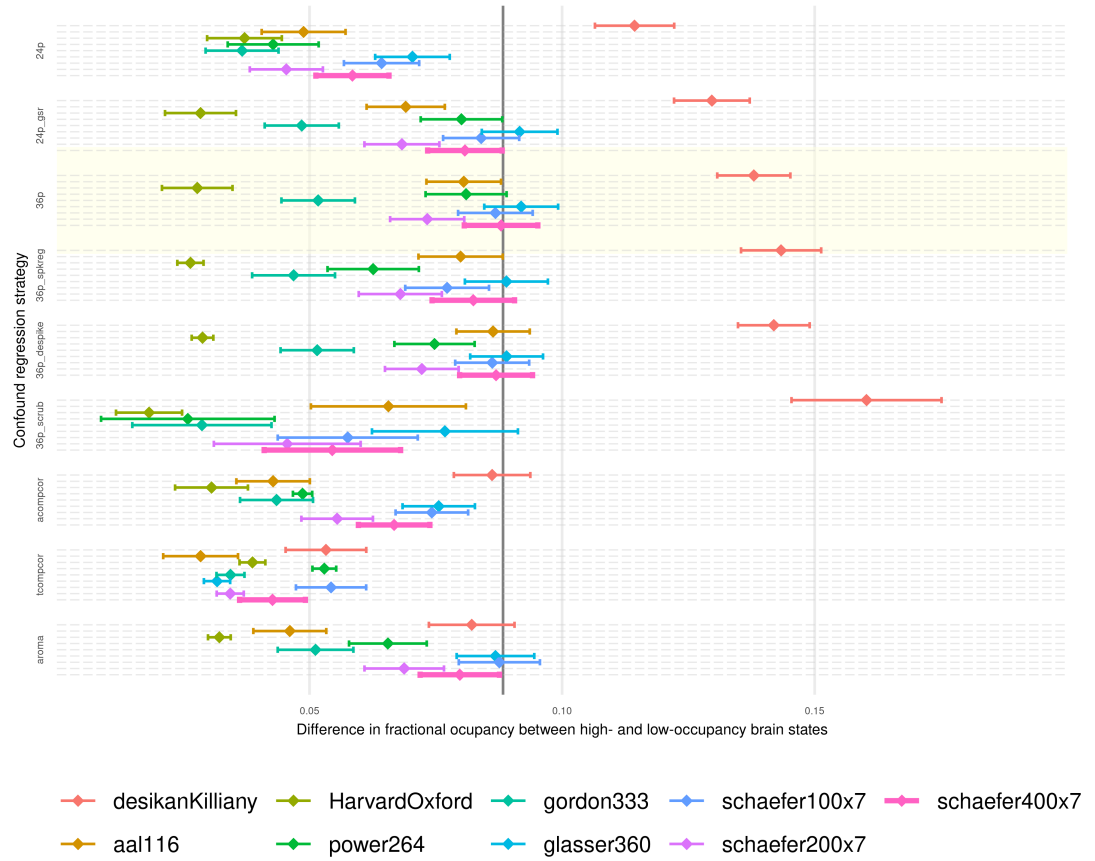


Figure 2. Point estimates (dots) and 95 % confidence intervals (line segments) for the mean difference in fractional occupancy between high- and low occupancy states are shown for different confound regression strategies (groups along the vertical axis) and brain parcellations (color). The difference in FO for a particular choice of regression strategy and brain parcellation is nominally statistically significantly different from zero at a significance level of 5% if the corresponding interval does not contain zero. Hence, the FO difference is significant for all processing choices, reflecting the separation between high- und low-occupancy states. The primary choices (36p and schaefer400) are highlighted by a yellow box and thick pink line, respectively. The effect size reported in (Schlemm et al., 2022) is indicated by a vertical line at 0.08830623.

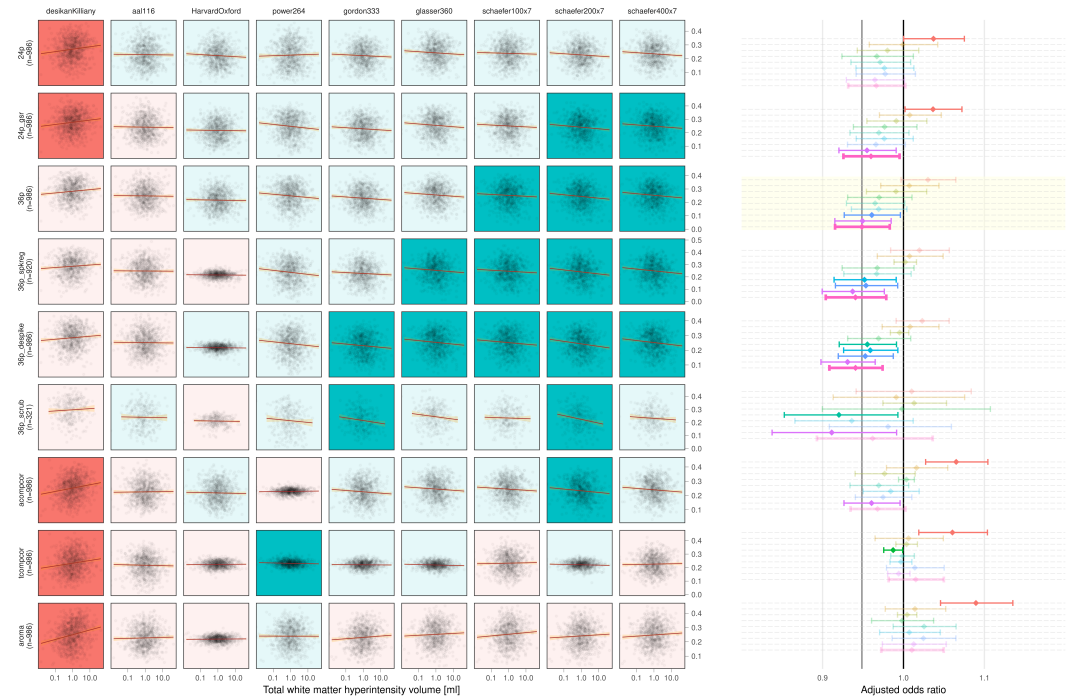


Figure 3. On the left, scatter plots of average fractional occupancies in high-occupancy states against WMH volume on a logarithmic scale (base 10 for easier visualization) for different combinations of confound regression strategies and brain parcellations. Linear regression lines indicate the direction of the unadjusted association between $\log(\text{WMH})$ and occupancy. Background color of individual panels indicates the direction of the association after adjustment for age, sex and zero WMH volume (green, negative; red, positive). A pale background indicates that the association between $\log(\text{WMH})$ and average occupancy is not statistically different from zero. On the right, the same information is shown using point estimates and 95 % confidence intervals for the adjusted odds ratio of the association.

252 Timeline and access to data

253 At the time of planning of this study, all demographic, clinical and imaging data used in
254 this analysis have been collected by the HCHS and are held in the central trial database.
255 Quality checks for non-imaging variables have been performed centrally. WMH segmen-
256 tation based on structural MRI data of the first 10 000 participants of the HCHS has been
257 performed previously using the BIANCA/LOCATE approach (Rimmele et al., 2022) and re-
258 sults are included in this preregistration ([./derivatives/WMH/cSVD_all.csv](#) [./derivatives/WMH/cS](#)).
259 Functional MRI data and clinical measures of executive dysfunction (TMT-B scores) have
260 not been analyzed by the author. Analysis of the data will begin immediately after acceptance-
261 in-principle of the stage 1 submission of the registered report is obtained. Submission
262 of the full manuscript (stage 2) is planned two months later.

263 Acknowledgment

264 This preprint was created using the LaPreprint template (<https://github.com/roaldarbol/>
265 [lapreprint](#)) by Mikkel Roald-Arbøl .

266 References

- 267 Arbuthnott, Katherine and Janis Frank (2000). "Trail making test, part B as a measure of
268 executive control: validation using a set-switching paradigm". In: *Journal of clinical and*
269 *experimental neuropsychology* 22.4, pp. 518–528.
- 270 Behzadi, Yashar et al. (2007). "A component based noise correction method (CompCor)
271 for BOLD and perfusion based fMRI". In: *Neuroimage* 37.1, pp. 90–101.
- 272 Bos, Daniel et al. (2018). "Cerebral small vessel disease and the risk of dementia: A sys-
273 tematic review and meta-analysis of population-based evidence". en. In: *Alzheimers.*
274 *Dement.* 14.11, pp. 1482–1492.
- 275 Cannistraro, Rocco J et al. (2019). "CNS small vessel disease: A clinical review". en. In: *Neu-*
276 *rology* 92.24, pp. 1146–1156.
- 277 Ceric, Rastko, Adon FG Rosen, et al. (2018). "Mitigating head motion artifact in functional
278 connectivity MRI". In: *Nature protocols* 13.12, pp. 2801–2826.
- 279 Ceric, Rastko, Daniel H Wolf, et al. (2017). "Benchmarking of participant-level confound
280 regression strategies for the control of motion artifact in studies of functional con-
281 nectivity". en. In: *Neuroimage* 154, pp. 174–187.

- 282 Cornblath, Eli J et al. (2020). "Temporal sequences of brain activity at rest are constrained
283 by white matter structure and modulated by cognitive demands". en. In: *Commun Biol*
284 3.1, p. 261.
- 285 Cox, Robert W (1996). "AFNI: software for analysis and visualization of functional mag-
286 netic resonance neuroimages". In: *Computers and Biomedical research* 29.3, pp. 162–
287 173.
- 288 Das, Alvin S et al. (2019). "Asymptomatic Cerebral Small Vessel Disease: Insights from
289 Population-Based Studies". en. In: *J. Stroke Cerebrovasc. Dis.* 21.2, pp. 121–138.
- 290 Desikan, Rahul S et al. (2006). "An automated labeling system for subdividing the human
291 cerebral cortex on MRI scans into gyral based regions of interest". In: *Neuroimage* 31.3,
292 pp. 968–980.
- 293 Dey, Ayan K et al. (2016). "Pathoconnectomics of cognitive impairment in small vessel
294 disease: A systematic review". en. In: *Alzheimers. Dement.* 12.7, pp. 831–845.
- 295 Esteban, Oscar et al. (2019). "fMRIprep: a robust preprocessing pipeline for functional
296 MRI". en. In: *Nat. Methods* 16.1, pp. 111–116.
- 297 Frey, Benedikt M et al. (2021). "White matter integrity and structural brain network topol-
298 ogy in cerebral small vessel disease: The Hamburg city health study". en. In: *Hum. Brain
299 Mapp.* 42.5, pp. 1406–1415.
- 300 Friston, Karl J et al. (1996). "Movement-related effects in fMRI time-series". In: *Magnetic
301 resonance in medicine* 35.3, pp. 346–355.
- 302 Gesierich, Benno et al. (2020). "Alterations and test-retest reliability of functional connec-
303 tivity network measures in cerebral small vessel disease". en. In: *Hum. Brain Mapp.*
304 41.10, pp. 2629–2641.
- 305 Glasser, Matthew F et al. (2016). "A multi-modal parcellation of human cerebral cortex".
306 en. In: *Nature* 536.7615, pp. 171–178.
- 307 Gordon, Evan M et al. (2016). "Generation and Evaluation of a Cortical Area Parcellation
308 from Resting-State Correlations". en. In: *Cereb. Cortex* 26.1, pp. 288–303.
- 309 Griffanti, Ludovica, Mark Jenkinson, et al. (2018). "Classification and characterization of
310 periventricular and deep white matter hyperintensities on MRI: A study in older adults".
311 en. In: *Neuroimage* 170, pp. 174–181.
- 312 Griffanti, Ludovica, Giovanna Zamboni, et al. (2016). "BIANCA (Brain Intensity AbNormal-
313 ity Classification Algorithm): A new tool for automated segmentation of white matter
314 hyperintensities". en. In: *Neuroimage* 141, pp. 191–205.

- ³¹⁵ Jagodzinski, Annika et al. (2020). "Rationale and Design of the Hamburg City Health Study".
³¹⁶ en. In: *Eur. J. Epidemiol.* 35.2, pp. 169–181.
- ³¹⁷ Laumann, Timothy O, Evan M Gordon, et al. (2015). "Functional system and areal organi-
³¹⁸ zation of a highly sampled individual human brain". In: *Neuron* 87.3, pp. 657–670.
- ³¹⁹ Laumann, Timothy O and Abraham Z Snyder (2021). "Brain activity is not only for thinking".
³²⁰ In: *Current Opinion in Behavioral Sciences* 40, pp. 130–136.
- ³²¹ Laumann, Timothy O, Abraham Z Snyder, et al. (2017). "On the stability of BOLD fMRI
³²² correlations". In: *Cerebral cortex* 27.10, pp. 4719–4732.
- ³²³ Lawrence, Andrew J, Ai Wern Chung, et al. (2014). "Structural network efficiency is as-
³²⁴ sociated with cognitive impairment in small-vessel disease". en. In: *Neurology* 83.4,
³²⁵ pp. 304–311.
- ³²⁶ Lawrence, Andrew J, Daniel J Tozer, et al. (2018). "A comparison of functional and trac-
³²⁷ tography based networks in cerebral small vessel disease". en. In: *Neuroimage Clin* 18,
³²⁸ pp. 425–432.
- ³²⁹ Lawrence, Andrew J, Eva A Zeestraten, et al. (2018). "Longitudinal decline in structural
³³⁰ networks predicts dementia in cerebral small vessel disease". en. In: *Neurology* 90.21,
³³¹ e1898–e1910.
- ³³² Macey, Paul M et al. (2004). "A method for removal of global effects from fMRI time series".
³³³ In: *Neuroimage* 22.1, pp. 360–366.
- ³³⁴ Makris, Nikos et al. (2006). "Decreased volume of left and total anterior insular lobule in
³³⁵ schizophrenia". In: *Schizophrenia research* 83.2-3, pp. 155–171.
- ³³⁶ Muschelli, John et al. (2014). "Reduction of motion-related artifacts in resting state fMRI
³³⁷ using aCompCor". In: *Neuroimage* 96, pp. 22–35.
- ³³⁸ Petersen, Marvin et al. (2020). "Network Localisation of White Matter Damage in Cerebral
³³⁹ Small Vessel Disease". en. In: *Sci. Rep.* 10.1, p. 9210.
- ³⁴⁰ Power, Jonathan D, Alexander L Cohen, et al. (2011). "Functional network organization of
³⁴¹ the human brain". en. In: *Neuron* 72.4, pp. 665–678.
- ³⁴² Power, Jonathan D, Anish Mitra, et al. (2014). "Methods to detect, characterize, and re-
³⁴³ move motion artifact in resting state fMRI". In: *Neuroimage* 84, pp. 320–341.
- ³⁴⁴ Prins, Niels D et al. (2005). "Cerebral small-vessel disease and decline in information pro-
³⁴⁵ cessing speed, executive function and memory". en. In: *Brain* 128.Pt 9, pp. 2034–2041.
- ³⁴⁶ Pruim, Raimon HR et al. (2015). "ICA-AROMA: A robust ICA-based strategy for removing
³⁴⁷ motion artifacts from fMRI data". In: *Neuroimage* 112, pp. 267–277.

- ³⁴⁸ Reijmer, Yael D et al. (2016). "Small vessel disease and cognitive impairment: The relevance of central network connections". en. In: *Hum. Brain Mapp.* 37.7, pp. 2446–2454.
- ³⁴⁹
- ³⁵⁰ Rimmele, David Leander et al. (2022). "Association of Carotid Plaque and Flow Velocity With White Matter Integrity in a Middle-aged to Elderly Population". en. In: *Neurology*.
- ³⁵¹
- ³⁵² Satterthwaite, Theodore D et al. (2013). "An improved framework for confound regression and filtering for control of motion artifact in the preprocessing of resting-state functional connectivity data". In: *Neuroimage* 64, pp. 240–256.
- ³⁵³
- ³⁵⁴
- ³⁵⁵ Schaefer, Alexander et al. (2018). "Local-Global Parcellation of the Human Cerebral Cortex from Intrinsic Functional Connectivity MRI". en. In: *Cereb. Cortex* 28.9, pp. 3095–3114.
- ³⁵⁶
- ³⁵⁷ Schlemm, Eckhard et al. (2022). "Equalization of Brain State Occupancy Accompanies Cognitive Impairment in Cerebral Small Vessel Disease". en. In: *Biol. Psychiatry* 92.7, pp. 592–602.
- ³⁵⁸
- ³⁵⁹
- ³⁶⁰ Schulz, Maximilian et al. (2021). "Functional connectivity changes in cerebral small vessel disease - a systematic review of the resting-state MRI literature". en. In: *BMC Med.* 19.1, p. 103.
- ³⁶¹
- ³⁶²
- ³⁶³ Shen, Jun et al. (2020). "Network Efficiency Mediates the Relationship Between Vascular Burden and Cognitive Impairment: A Diffusion Tensor Imaging Study in UK Biobank". en. In: *Stroke* 51.6, pp. 1682–1689.
- ³⁶⁴
- ³⁶⁵
- ³⁶⁶ Steegen, Sara et al. (2016). "Increasing Transparency Through a Multiverse Analysis". en. In: *Perspect. Psychol. Sci.* 11.5, pp. 702–712.
- ³⁶⁷
- ³⁶⁸ Sundaresan, Vaanathi et al. (2019). "Automated lesion segmentation with BIANCA: Impact of population-level features, classification algorithm and locally adaptive thresholding". en. In: *Neuroimage* 202, p. 116056.
- ³⁶⁹
- ³⁷⁰
- ³⁷¹ Tombaugh, Tom N (2004). "Trail Making Test A and B: normative data stratified by age and education". en. In: *Arch. Clin. Neuropsychol.* 19.2, pp. 203–214.
- ³⁷²
- ³⁷³ Tuladhar, Anil M, Ewoud van Dijk, et al. (2016). "Structural network connectivity and cognition in cerebral small vessel disease". en. In: *Hum. Brain Mapp.* 37.1, pp. 300–310.
- ³⁷⁴
- ³⁷⁵ Tuladhar, Anil M, Jonathan Tay, et al. (2020). "Structural network changes in cerebral small vessel disease". en. In: *J. Neurol. Neurosurg. Psychiatry* 91.2, pp. 196–203.
- ³⁷⁶
- ³⁷⁷ Tzourio-Mazoyer, Nathalie et al. (2002). "Automated anatomical labeling of activations in SPM using a macroscopic anatomical parcellation of the MNI MRI single-subject brain". In: *Neuroimage* 15.1, pp. 273–289.
- ³⁷⁸
- ³⁷⁹

- ³⁸⁰ Vidaurre, Diego et al. (2018). "Discovering dynamic brain networks from big data in rest
³⁸¹ and task". en. In: *Neuroimage* 180.Pt B, pp. 646–656.
- ³⁸² Wardlaw, Joanna M, Colin Smith, and Martin Dichgans (2013). "Mechanisms of sporadic
³⁸³ cerebral small vessel disease: insights from neuroimaging". en. In: *Lancet Neurol.* 12.5,
³⁸⁴ pp. 483–497.
- ³⁸⁵ Wardlaw, Joanna M, Eric E Smith, et al. (2013). "Neuroimaging standards for research
³⁸⁶ into small vessel disease and its contribution to ageing and neurodegeneration". en.
³⁸⁷ In: *Lancet Neurol.* 12.8, pp. 822–838.
- ³⁸⁸ Wardlaw, Joanna M, María C Valdés Hernández, and Susana Muñoz-Maniega (2015). "What
³⁸⁹ are white matter hyperintensities made of? Relevance to vascular cognitive impairment". en. In: *J. Am. Heart Assoc.* 4.6, p. 001140.
- ³⁹⁰ Xu, Yuanhang et al. (2021). "Altered Dynamic Functional Connectivity in Subcortical Is-
³⁹¹ chemic Vascular Disease With Cognitive Impairment". en. In: *Front. Aging Neurosci.* 13,
³⁹² p. 758137.
- ³⁹³ Yeo, B T Thomas et al. (2011). "The organization of the human cerebral cortex estimated
³⁹⁴ by intrinsic functional connectivity". en. In: *J. Neurophysiol.* 106.3, pp. 1125–1165.
- ³⁹⁵ Yin, Wenwen et al. (2022). "The Clustering Analysis of Time Properties in Patients With
³⁹⁶ Cerebral Small Vessel Disease: A Dynamic Connectivity Study". en. In: *Front. Neurol.*
³⁹⁷ 13, p. 913241.